Stem Cell Reports
Article

OPEN ACCESS

Latexin Inactivation Enhances Survival and Long-Term Engraftment of Hematopoietic Stem Cells and Expands the Entire Hematopoietic System in Mice

Yi Liu,[2] Cuiping Zhang,[1] Zhenyu Li,[3] Chi Wang,[4] Jianhang Jia,[5] Tianyan Gao,[5] Gerhard Hildebrandt,[3] Daohong Zhou,[6] Subbarao Bondada,[7] Peng Ji,[8] Daret St. Clair,[1] Jinze Liu,[9] Changguo Zhan,[10] Hartmut Geiger,[11,12] Shuxia Wang,[13] and Ying Liang[1,*]

[1]Department of Toxicology and Cancer Biology, University of Kentucky, Health Sciences Research Building Room 340, 1095 V.A. Drive, Lexington, KY 40536, USA
[2]Department of Physiology
[3]Department of Internal Medicine
[4]Department of Cancer Biostatistics
[5]Department of Molecular & Cellular Biochemistry
University of Kentucky, Lexington, KY 40536, USA
[6]Division of Radiation Health, Department of Pharmaceutical Sciences, University of Arkansas for Medical Sciences, Little Rock, AR 72205, USA
[7]Department of Microbiology, Immunology and Molecular Genetics, University of Kentucky, Lexington, KY 40536, USA
[8]Department of Pathology, Northwestern University, Chicago, IL 60611, USA
[9]Department of Computer Science
[10]Department of Pharmaceutical Sciences
University of Kentucky, Lexington, KY 40536, USA
[11]Cincinnati Children's Hospital Medical Center, Experimental Hematology and Cancer Biology, Cincinnati, OH 45229, USA
[12]Institute for Molecular Medicine, University of Ulm, 89081 Ulm, Germany
[13]Department of Pharmacology and Nutritional Sciences, University of Kentucky, Lexington, KY 40536, USA
*Correspondence: ying.liang@uky.edu
http://dx.doi.org/10.1016/j.stemcr.2017.02.009

SUMMARY

Natural genetic diversity offers an important yet largely untapped resource to decipher the molecular mechanisms regulating hematopoietic stem cell (HSC) function. Latexin (*Lxn*) is a negative stem cell regulatory gene identified on the basis of genetic diversity. By using an Lxn knockout mouse model, we found that *Lxn* inactivation in vivo led to the physiological expansion of the entire hematopoietic hierarchy. Loss of *Lxn* enhanced the competitive repopulation capacity and survival of HSCs in a cell-intrinsic manner. Gene profiling of *Lxn*-null HSCs showed altered expression of genes enriched in cell-matrix and cell-cell interactions. Thrombospondin 1 (*Thbs1*) was a potential downstream target with a dramatic downregulation in *Lxn*-null HSCs. Enforced expression of *Thbs1* restored the *Lxn* inactivation-mediated HSC phenotypes. This study reveals that *Lxn* plays an important role in the maintenance of homeostatic hematopoiesis, and it may lead to development of safe and effective approaches to manipulate HSCs for clinical benefit.

INTRODUCTION

Hematopoietic stem cells (HSCs) persist throughout life to produce hematopoietic progenitor cells (HPCs) and all types of blood cells. In the adult, HSCs reside in bone marrow (BM), are rare but have the unique capability for self-renewal and multilineage differentiation (Eaves, 2015). The maintenance of a steady-state HSC pool adept at dynamic change in response to stress depends on the balance of self-renewal, differentiation, survival, and proliferation (Goodell et al., 2015). Loss of this balance could lead to an overexpansion or exhaustion of HSC population, and result in an increased risk for cancer or tissue degeneration. HSCs have been used therapeutically in the clinic for several decades in life-saving treatment of malignant diseases and hematological disorders through BM transplantation protocols (Doulatov et al., 2012). However, insufficient stem cell numbers significantly limit the efficacy and success of these regimes. Expansion of HSCs while maintaining their self-renewal capability has been one of the most desired, yet elusive, goals in experimental hematology and transplantation medicine (Walasek et al., 2012).

HSC fate decisions require strict control. Multiple signaling pathways regulate HSC functions through cell-intrinsic and cell-extrinsic mechanisms (Rossi et al., 2012; Gottgens, 2015). Genetic manipulation of transcription factors and signal transduction pathways enhances HSC expansion ex vivo (Andrade et al., 2010, 2011); these include the homeobox gene family (Antonchuk et al., 2002), immobilized Notch ligand (Delaney et al., 2010), Wnt-associated prostaglandin E2 (Goessling et al., 2011), the soluble growth factors angiopoietin-like 5 (Zheng et al., 2012), pleiotrophin (Himburg et al., 2010; Himburg et al., 2012), and miR-126 (Lechman et al., 2012), and the aryl hydrocarbon receptor inhibitor (Boitano et al., 2010). Moreover, employing an induced pluripotent stem cell population and targeting the HSC microenvironment hold promise for HSC expansion (Blanpain et al., 2012;

Kunisaki and Frenette, 2012; Huang et al., 2013; Chen et al., 2014). However, all these attempts have had limited success clinically, due to a failure to expand sustainable and self-renewable stem cells (Walasek et al., 2012).

Our understanding of the molecular pathways for HSC fate decision is insufficient to allow safe manipulation of HSCs for clinical benefit. Large natural variations in HSC number and function exist in humans (Nathan and Orkin, 2009; Sankaran and Orkin, 2013) as well as in different mouse strains (Jordan and Van Zant, 1998; Geiger et al., 2001; Henckaerts et al., 2002; Abiola et al., 2003; Hsu et al., 2007; Cahan et al., 2009; Avagyan et al., 2011). Such natural genetic diversity is an important yet largely unused tool for unraveling the genes and signaling networks associated with stem cell regulation (Van Zant and Liang, 2009). Using this genetic diversity tool, we previously identified latexin (*Lxn*) as a stem cell regulatory gene with expression that negatively correlates with HSC number variation in different mouse strains (de Haan, 2007; Liang et al., 2007). *Lxn* is a negative regulator of HSC function and works as a "brake" to constrain the HSC pool to a physiological range. In addition, the canonical function of *Lxn* protein is its inhibitory effect of carboxypeptidase A (Liu et al., 2000; Uratani et al., 2000; Pallares et al., 2005; Mouradov et al., 2006). Studies have also shown that LXN has high structural similarity with cystatin and tumor suppressor TIG1 gene, suggesting its potential role in inflammation and transformation (Aagaard et al., 2005). However, the in vivo function of *Lxn* in hematopoiesis and the underlying regulatory cellular and molecular mechanisms remain largely elusive. Particularly, when drawing upon genetic diversity to identify genes (usually multiple ones) associated with a complex trait (HSC number), all contributing genes are important (Van Zant and Liang, 2009). Therefore, it warrants to know to what extent *Lxn* contributes to the natural variation of the size of HSC population and how it specifically regulates HSC function and hematopoiesis.

In this study, we showed that *Lxn* deletion in vivo leads to increased numbers of HSCs, HPCs, and all blood cell lineages. Loss of *Lxn* enhanced long-term repopulating capacity and survival of HSCs. Mechanistically, gene array analysis showed that genes involved in cell-cell and cell-matrix interaction were dysregulated in $Lxn^{-/-}$ HSCs, and thrombospondin 1 (*Thbs1*) was identified as a potential downstream target of *Lxn*. *Thbs1* mRNA and protein levels were significantly decreased in $Lxn^{-/-}$ HSCs, and ectopic expression of *Thbs1* rescued the $Lxn^{-/-}$ HSC phenotype. Our study reveals the cellular and molecular regulatory mechanisms of *Lxn* in HSC homeostasis, and highlights the importance of *Lxn*-mediated intrinsic and extrinsic cellular signaling in the control of HSC function.

RESULTS

$Lxn^{-/-}$ Mice Have Increased Blood Cell Numbers and Balanced Lineage Differentiation

The constitutive *Lxn* knockout ($Lxn^{-/-}$) mice were generated on the C57BL/6 background. Because Lxn gene lies within the mitochondrial elongation factor G (*Gfm1*) gene, only exons 2 to 4 were targeted for deletion to minimize any potential effect on *Gfm1* (Figure 1A). Western blot showed complete deletion of the LXN protein in BM, spleen, liver, and brain without affecting GFM1 protein expression (Figure 1B). Peripheral blood (PB) analysis of $Lxn^{-/-}$ mice showed a significant increase in the counts of complete white blood cells, neutrophils, monocytes, lymphocytes, and platelets compared with those of wild-type (WT) mice (Figure 1C). The percentages of macrophages, granulocytes (Mac-1/Gr-1+), and B lymphocytes (B220+) in $Lxn^{-/-}$ mice showed a slight but significant increase (Figure 1D), whereas the T lineage was not affected (data not shown). These data suggest that *Lxn* deletion increases the number of mature blood cells of both myeloid and lymphoid lineages without skewing differentiation.

Lxn Inactivation Leads to Expansion of the HSC and HPC Populations

Analysis of the BM compartment of $Lxn^{-/-}$ mice showed a significant increase in cellularity compared with WT mice (Figure 2A), despite similar body weights (data not shown). Using flow cytometry and immunostaining of HSCs and HPCs (Figure 2B), we found that the absolute numbers of HPCs, including common myeloid progenitor (CMP), granulocyte/monocyte progenitor (GMP), and common lymphoid progenitor (CLP) cells, were significantly increased in $Lxn^{-/-}$ mice (Figure 2C). Moreover, $Lxn^{-/-}$ mice consistently presented a 56% increase in the absolute number of HSC/HPC-enriched LSK cells (Figure 3D). Among the LSK population, the absolute numbers of long-term (LT)-HSCs, short-term (ST)-HSCs, and multipotent progenitor cells (MPPs) were all significantly increased in $Lxn^{-/-}$ mice compared with WT mice (Figures 2E–2G). These data suggest that *Lxn* inactivation leads to an expansion of the hematopoietic stem and progenitor pool, which contributes to the increased blood cell counts.

Lxn Inactivation Increases HSC Clonogenic and Repopulating Capacity in a Cell-Intrinsic Manner

To define the effect of *Lxn* inactivation on the function of HSCs and HPCs, we used the in vitro culture system, including cobblestone area-forming cell (CAFC) and colony-forming cell (CFC) assays, to assess the clonogenic potential of HSCs and HPCs, respectively. Figure 3A shows that the number of primitive HSCs (CAFC day 35) was

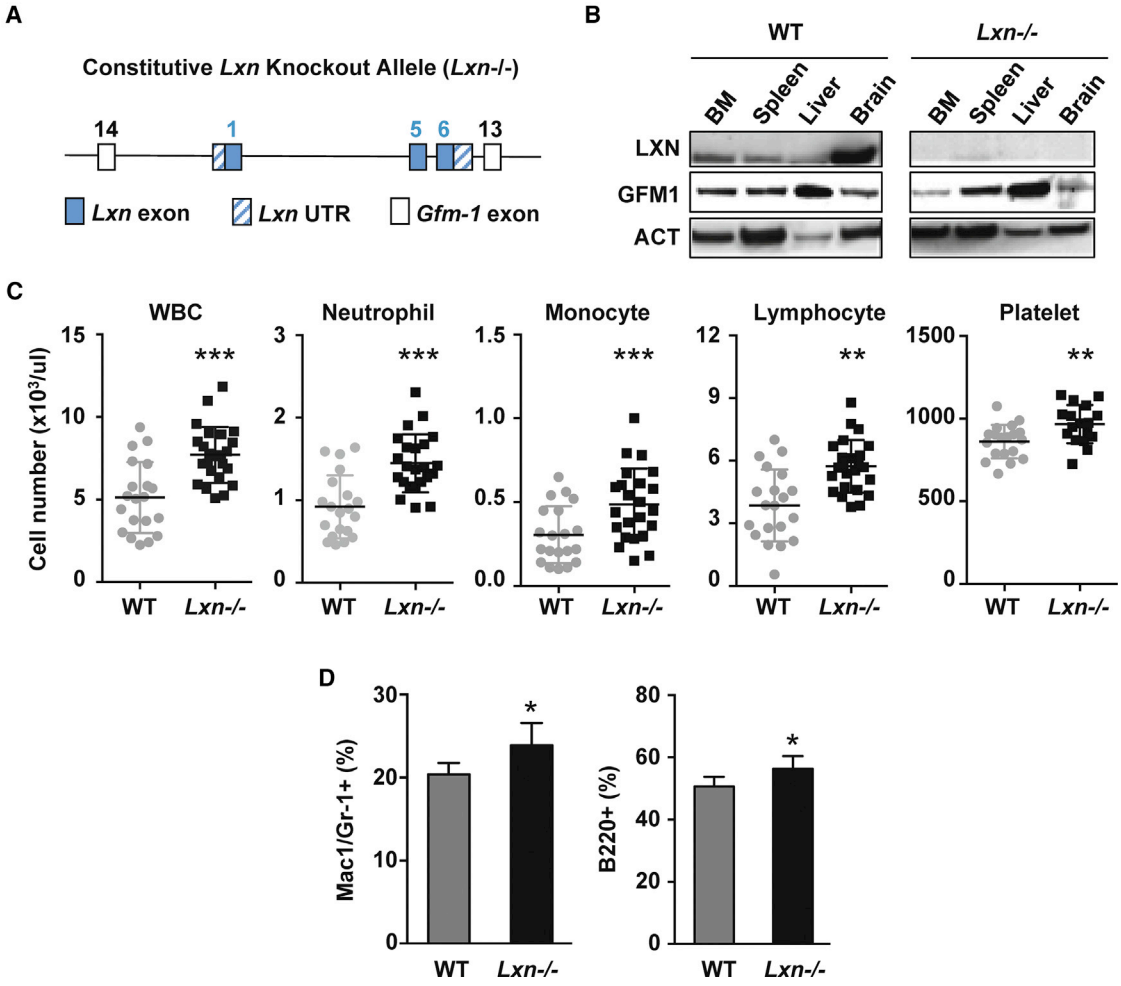

Figure 1. *Lxn* Inactivation Increases Peripheral Blood Cell Numbers

(A) Scheme representing the *Lxn* gene targeting strategy. The *Lxn* gene lies within the *Gfm-1* gene and only exons 2 to 4 of the *Lxn* gene were removed to minimize any potential effect on the *Gfm-1* gene.

(B) Western blot analysis of *Lxn* and *Gfm-1* protein from the indicated organs of $Lxn^{-/-}$ and WT control mice.

(C) Differential blood cell counts of $Lxn^{-/-}$ and WT mice. Statistically significant differences are: ***$p < 0.001$, **$p < 0.01$.

(D) Lineage differentiation analysis by immunostaining and flow cytometry of $Lxn^{-/-}$ and WT myeloid cells (MAC1/GR1+) and B lymphocytes (B220+). *$p < 0.01$. Presented data in (C and D) are the mean ± SD from three independent experiments (n = 22 in $Lxn^{-/-}$, n = 20 in WT mice).

3-fold higher in $Lxn^{-/-}$ BM than WT BM. Moreover, the total number of CFCs generated by $Lxn^{-/-}$ BM cells was increased by nearly 2-fold compared with WT cells (Figure 3B). We next evaluated the capability of $Lxn^{-/-}$ HSCs to reconstitute the hematopoiesis of myeloablated mice by a competitive repopulation assay (Figure 3C). The results showed that $Lxn^{-/-}$ HSCs made a greater contribution to the repopulation of PB leukocytes at both 8 weeks and 16 weeks post transplantation compared with WT cells (Figure 3D). Analysis of PB lineage chimerism at 16 weeks showed that the engrafted $Lxn^{-/-}$ HSCs retained multilineage differentiation potential and contributed to more circulating myeloid and B cells than the WT cells (Figure 3E). This recapitulates the intrinsic changes of $Lxn^{-/-}$ cells in physiological condition (Figure 1D). Analysis of BM chimerism showed that mice transplanted with $Lxn^{-/-}$ cells presented with 66.4% (±9.9%) donor-derived cells, whereas in mice receiving WT cells, the contribution was dramatically lower at 30.9% (±16.9%) (Figure 3F). In the BM LSK compartment, the percentage and absolute number of $Lxn^{-/-}$-derived LSK cells was nearly 3-fold higher than that of WT-derived cells (Figures 3G and 3H, respectively). Altogether, these results reinforce findings of increased numbers of functional HSC and HPC, as measured by their

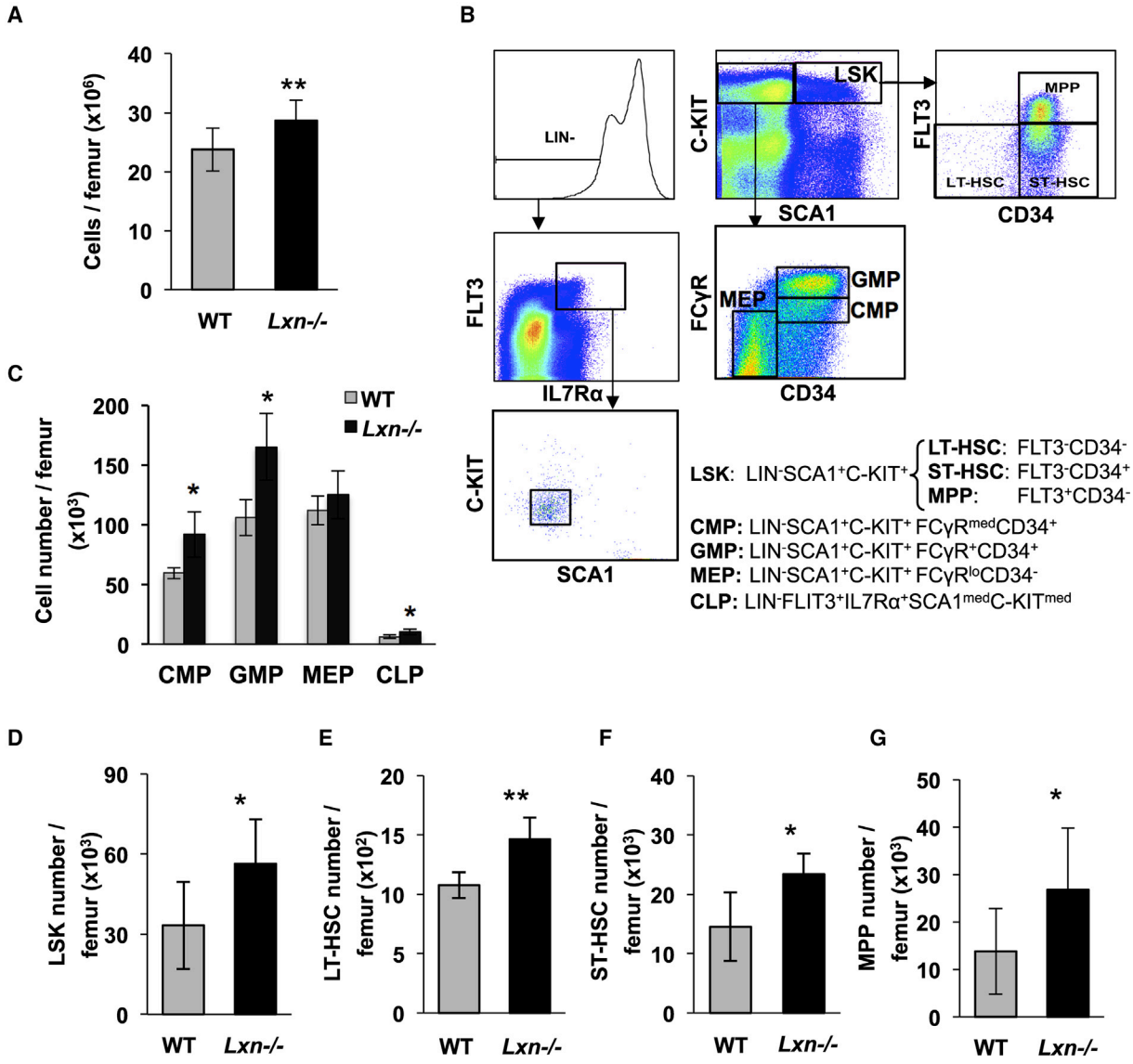

Figure 2. *Lxn* Inactivation Expands the Immunophenotypically Defined HSCs and HPCs

(A) Total femoral BM cell counts (cellularity) of $Lxn^{-/-}$ (n = 22) and WT (n = 20) mice. **p = 0.002.

(B) Representative FACS plots for HSC and HPC cell populations, including HSC and HPC-enriched LSK cells, HSC subsets (LT-HSCs, ST-HSCs, and MPPs), myeloid committed progenitor cells (CMPs, GMPs, and MEPs), and common lymphoid progenitor cells (CLPs). Cell surface makers for identification of each cell populations are indicated.

(C) Absolute number of CMPs (*p = 0.03), GMPs (*p = 0.02), MEPs, and CLPs (*p = 0.04) in one femur of an $Lxn^{-/-}$ and a WT mouse.

(D) Absolute number of LSK cells in one femur of an $Lxn^{-/-}$ and a WT mouse. *p = 0.046.

(E–G) Absolute number of LT-HSCs (**p = 0.003), ST-HSCs (*p = 0.02), and MPP cells (*p = 0.048) in one femur of an $Lxn^{-/-}$ and a WT mouse.

Presented data in (A–G) are the average ± SD pooled from three independent experiments with three mice per experiment for both strains (n = 9 each strain).

clonogenic activity in $Lxn^{-/-}$ mice. The data suggest that *Lxn* inactivation significantly enhances HSC long-term reconstitution capacity and maintains multilineage differentiation potential in a cell-intrinsic manner. Moreover, the extent of expansion of $Lxn^{-/-}$-derived LSK population in this transplantation setting (3-fold) is higher than that in in situ condition (1-fold, Figure 2D), indicating the likelihood of increased self-renewal of $Lxn^{-/-}$ HSCs. Future studies are needed to address this by the serial transplantability of $Lxn^{-/-}$ HSCs.

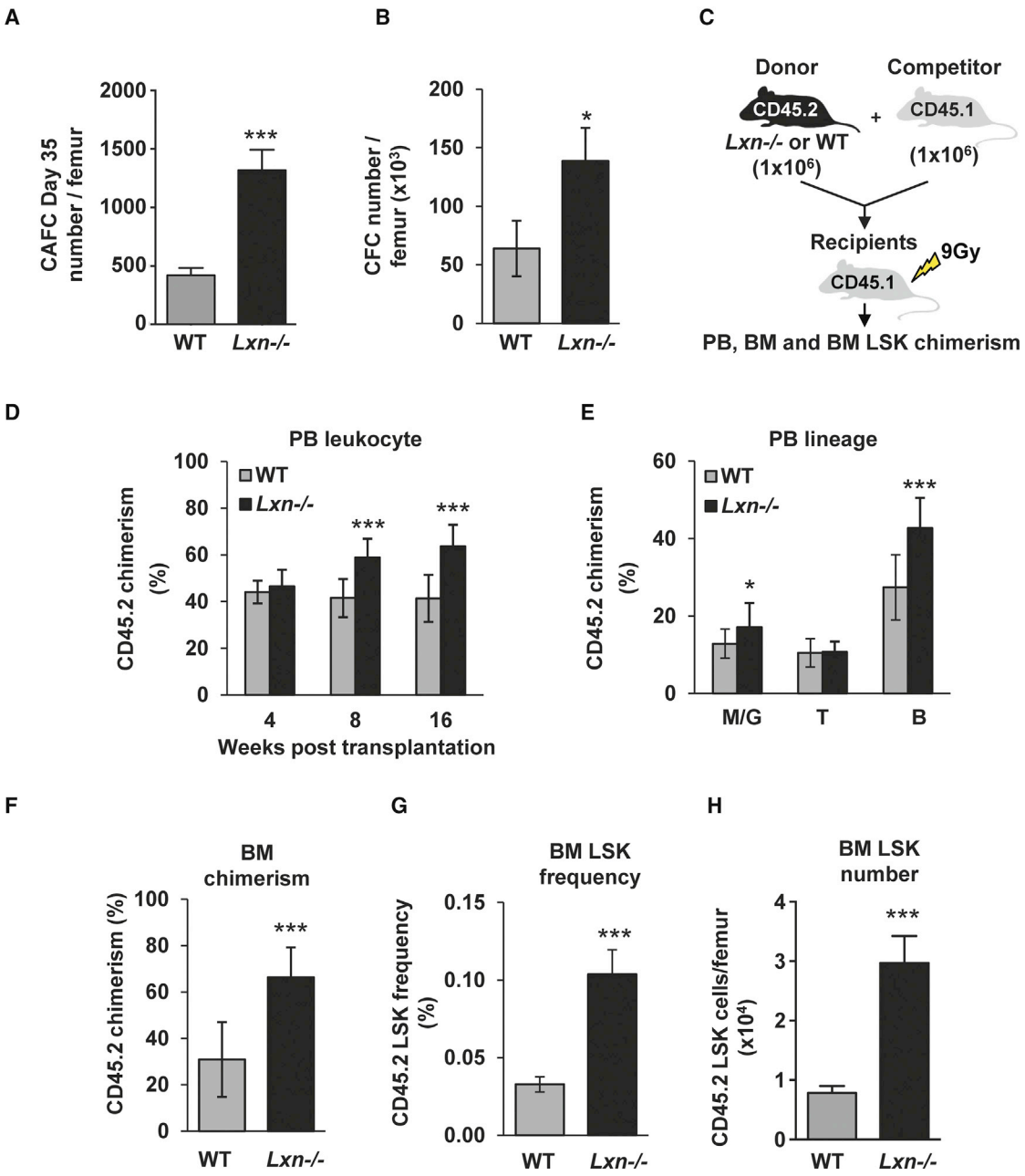

Figure 3. *Lxn* Inactivation Increases the Number of Functional HSCs and HPCs, and Enhances the Competitive Repopulation Capacity of HSCs

(A) Absolute number of clones, defined by the cobblestone area-forming cell (CAFC) assay, at d35 of culture for HSC cells from $Lxn^{-/-}$ and WT mice (***p = 0.0002).

(B) Absolute number of clones, defined by colony-forming cell (CFC) assay, at day 14 of culture for HPC cells from $Lxn^{-/-}$ and WT mice (*p = 0.01). Presented data are the average ±SD pooled from three independent experiments with three mice per experiment for both strains (n = 9 each strain).

(C) Experimental scheme for competitive repopulation assay.

(D–H) Frequencies of $Lxn^{-/-}$ or WT donor (CD45.2)-derived leukocytes at 4, 8, and 16 (***p < 0.001) weeks after transplantation in the PB of recipient mice (CD45.1). At 16 weeks after transplantation in the BM of recipient mice, frequencies of $Lxn^{-/-}$ or WT donor

(legend continued on next page)

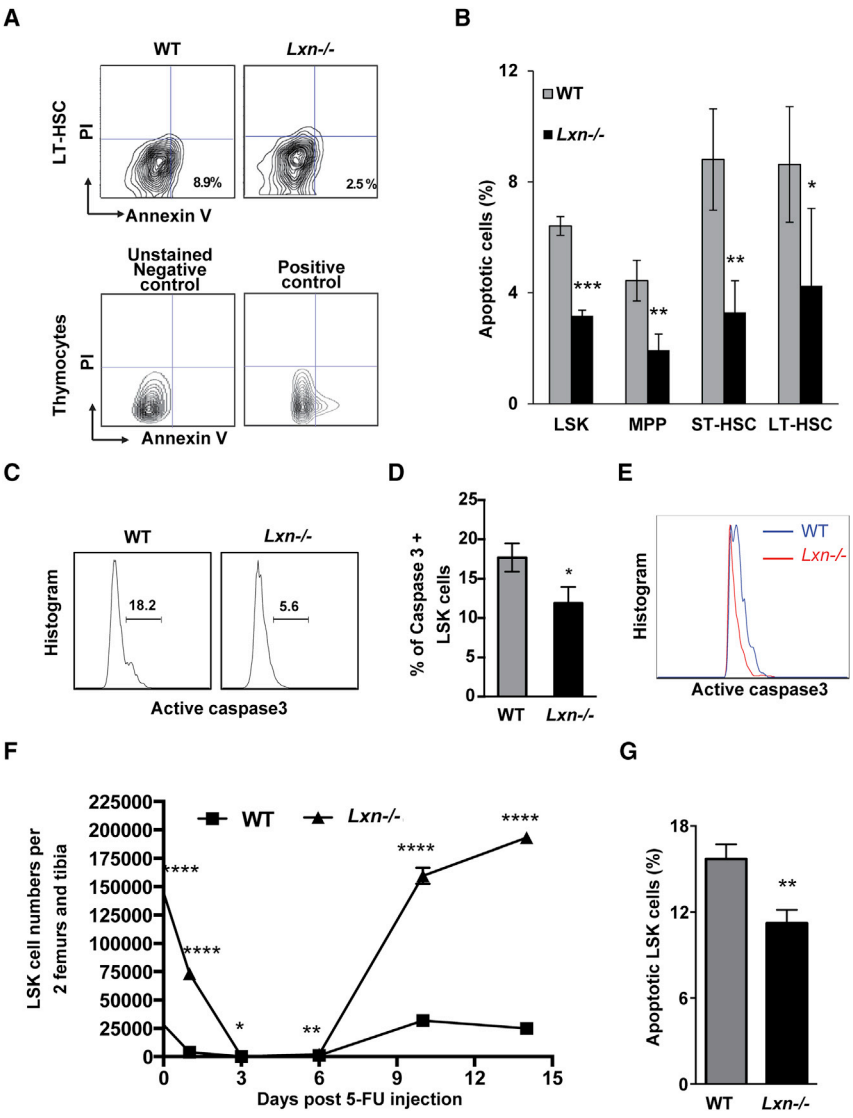

Figure 4. *Lxn*$^{-/-}$ HSCs have Increased Survival

(A) Representative FACS plots of Annexin V+ and 7-AAD apoptotic LT-HSCs (left plots). Thymocytes were used as control to determine the Annexin V+ population, as we published previously (Liang et al., 2007).

(B) Percentage of apoptotic cells in populations of LSK cells, MPPs, ST-HSCs, and LT-HSCs of *Lxn*$^{-/-}$ and WT mice. Presented data are the average ± SD of five mice/group.

(C) Representative flow cytometry profile of active caspase-3 immunofluorescence signal in LSK cells.

(D) Frequency of LSK cells positive for active caspase-3 (*p = 0.04).

(E) The level of the active caspase-3 protein in LSK cells of WT and Lxn$^{-/-}$ mice. Shown is the histogram of active caspase-3 protein in flow cytometry analysis. Data were the average of three independent experiments with three mice in each one (n = 9).

(F) *Lxn*$^{-/-}$ mice had a faster recovery in LSK cells after 5-FU-induced hematopoietic stress at days 1, 3, 6, 10, and 14.

(G) Less *Lxn*$^{-/-}$ LSK cells underwent apoptosis at 24 hr after 5-FU injection.

Data were the average of five mice at each time point in each group. ****p < 0.0001, ***p < 0.001, **p < 0.01, and *p < 0.05.

Lxn Inactivation Enhances HSC Survival without Affecting Cell Cycling

The HSC pool size is maintained by the balance of apoptosis and proliferation. Apoptosis analysis with Annexin V showed that the percentage of Annexin V+ propidium iodide-negative (PI–) apoptotic cells (Figure 4A) was significantly decreased by nearly 50% in *Lxn*$^{-/-}$ LSK cells, and subsets of HSCs (LT-HSCs, ST-HSCs, and MPPs) compared with the WT cells (Figure 4B). Increased survival was further confirmed by flow cytometric analysis of LSK cells positive for active caspase-3 (Figure 4C). The percentage of positive cells was significantly lower in *Lxn*$^{-/-}$ mice than that in WT mice (Figure 4D). Moreover, expression of active caspase-3, as measured by the mean fluorescence intensity, was lower in *Lxn*$^{-/-}$ LSK cells than in WT cells (Figure 4E). These data suggest that *Lxn* inactivation can intrinsically enhance HSC survival. We further followed the response of WT and *Lxn*$^{-/-}$ HSCs to 5-fluorouracil (5-FU)-induced hematopoietic stress, and found that LSK cells in *Lxn*$^{-/-}$ BM recovered faster than that in WT mice

(CD45.2)-derived (E) myeloid cells (M/G; *p = 0.02), T and B lymphocytes (***p < 0.001), (F) BM nucleated (***p < 0.001), and (G) LSK cells (***p < 0.001), as well as (H) absolute numbers of LSK cells in one femur (***p < 0.001), were measured.

Presented data in (D–H) are the average ± SD pooled from two independent experiments with five recipients receiving either *Lxn*$^{-/-}$ or WT BM cells per experiment (n = 10 per donor group).

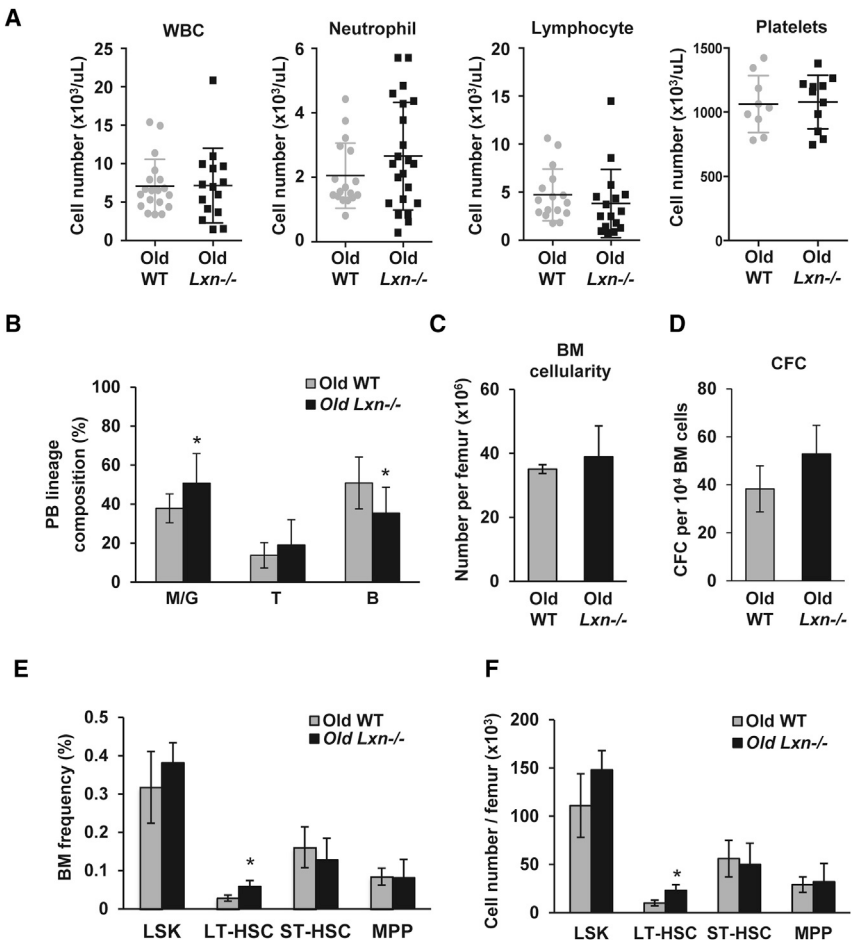

Figure 5. Aged *Lxn*$^{-/-}$ Mice Do Not Spontaneously Develop Hematologic Malignancy

In age-matched old *Lxn*$^{-/-}$ and WT mice, the following hematopoietic phenotypes were measured.

(A) Differential blood cell counts.

(B) Lineage differentiation analysis of myeloid cells (M/G; *p = 0.02) and T and B lymphocytes (*p = 0.03).

(C) Total BM cell counts (cellularity).

(D) Absolute number of CFC progenitor cell clones on day 14 of culture.

(E) Frequency of LSK cells, LT-HSCs (*p = 0.02), ST-HSCs, and MPPs in one femur.

(F) Absolute number of LSK cells, LT-HSCs (*p = 0.02), ST-HSCs, and MPPs in one femur.

Presented data in (A–F) are the average ± SD pooled from *Lxn*$^{-/-}$ (n = 15) and WT (n = 19) mice.

(Figure 4F), and less *Lxn*$^{-/-}$ LSK cells underwent apoptosis (Figure 4G). These results indicate that *Lxn* deletion protects hematopoietic stem/progenitor cells from 5FU-induced myelosuppression by enhancing their survival.

We next examined the cell-cycle status with Ki-67/PI staining and bromodeoxyuridine (BrdU) incorporation, and did not observe any significant difference in cell-cycle distribution and cycling dynamics between *Lxn*$^{-/-}$ and WT LT-HSCs (Figures S1A and S1B, respectively). This result suggests that *Lxn* did not affect stem cell cycling under physiological conditions.

Lxn$^{-/-}$ Mice Do Not Develop Hematological Malignancy during Aging

We and others have shown that *Lxn* is downregulated in leukemia, lymphoma, and several other cancers (Li et al., 2011; Liu et al., 2012; Mitsunaga et al., 2012; Abd Elmageed et al., 2013; Muthusamy et al., 2013; Ni et al., 2014). Since young *Lxn*$^{-/-}$ mice did not show any obvious sign of hematological malignancy, we asked whether aging could promote tumor development in *Lxn*$^{-/-}$ mice. Cohorts of *Lxn*$^{-/-}$ and WT mice were physiologically aged for 28 months and the hematopoietic profile in PB and BM was analyzed. No significant difference in either complete or differentiated blood cell counts was identified between aged-matched *Lxn*$^{-/-}$ and WT mice (Figure 5A). Lineage differentiation in old *Lxn*$^{-/-}$ mice showed a slight but significant increase in myeloid lineage and decrease in B lymphocytes (Figure 5B), although both strains demonstrated age-associated myeloid skewing and immunodeficiency compared with their young counterparts (Figure 1D). No significant difference was found in BM cellularity (Figure 5C) and the number of CFCs (Figure 5D). Aged *Lxn*$^{-/-}$ mice had nearly 2-fold more LT-HSCs in both frequency and absolute numbers than age-matched WT counterparts, but no significant difference was observed in other HSC sub-populations (Figures 5E and 5F). Importantly, the overall health of old *Lxn*$^{-/-}$ mice was comparable with the controls, and no apparent pathological changes were detected in blood, BM, spleen, and liver of *Lxn*$^{-/-}$ mice (data not shown). These data suggest that *Lxn*$^{-/-}$ mice are not inherently prone to hematological malignancy.

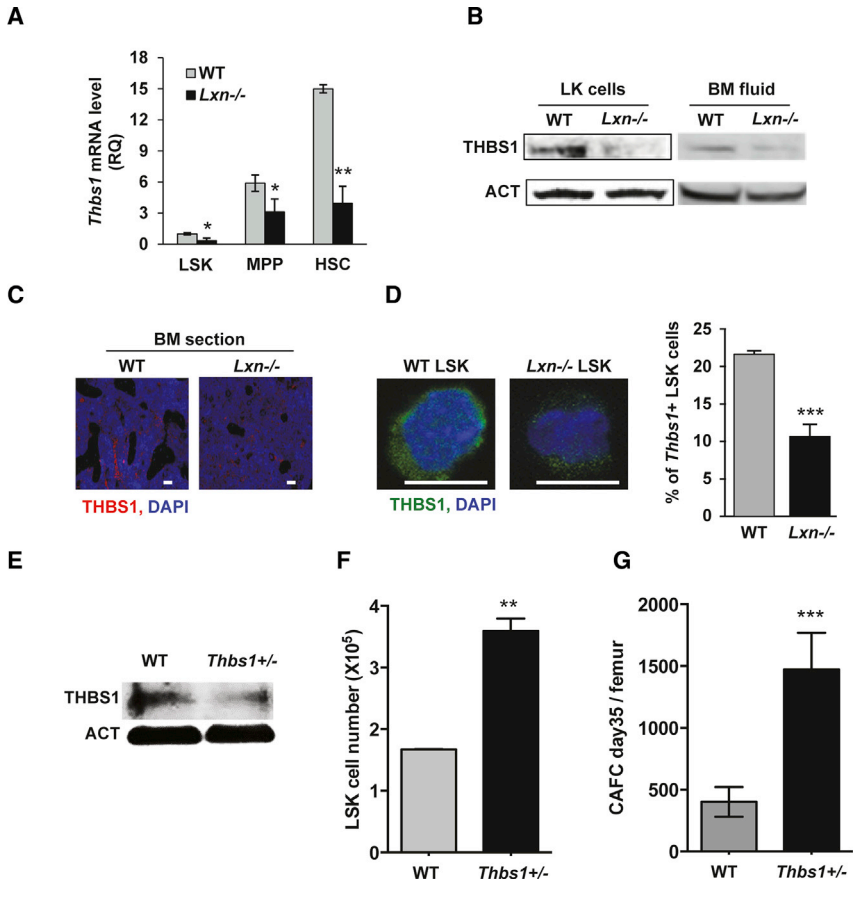

Figure 6. *Thbs1* Is the Downstream Target of *Lxn*

(A) Real-time PCR data demonstrating *Thbs1* mRNA levels in LSK, MPP, and HSCs. **p < 0.01 and *p < 0.05. HSCs are the combination of both LT-HSC and ST-HSCs (Lin– Sca1+ c-Kit+ Flt3 cells). Presented data are the average ±1 SD of 12 measurements derived from three separate samples.

(B) Western blot analysis of *Thbs1* protein in BM LIN-C-KIT+ (LK) cells and BM fluid. Actin (ACT) was normalization control. Blots are representative of three independent experiments.

(C) Immunofluorescence staining of the *Thbs1* protein (red) in BM sections from $Lxn^{-/-}$ and WT mice. Scale bars, 50 μm.

(D) Immunofluorescence staining of *Thbs1* protein (green) in individual $Lxn^{-/-}$ or WT LSK cells (left panel) and quantification of LSK cells positive for *Thbs1* staining (right panel). All cells (50–100) in the field were captured and analyzed in each sample. Scale bars, 5 μM. ***p = 0.0003.

(E) *Thbs1* heterozygous knockout mice ($Thbs1^{+/-}$) had reduced THBS1 levels. Western blot was performed on LSK cells and shown is one representative blot of two replicates.

(F) Increased number of LSK cells in $Thbs1^{+/-}$ BM. BM cells from $Thbs1^{+/-}$ mice were flow cytometrically analyzed for the LSK population. Data shown are the mean ±1 SD. **p = 0.01.

(G) Increased number of long-term colony-forming cells (CAFC day 35) in $Thbs1^{+/-}$ BM. Data shown are the mean ±1 SD. ***p = 0.003.

Thbs1 Is a Downstream Target of *Lxn*

We performed gene array analysis in phenotypically defined LT-HSCs and MPPs, respectively, to determine *Lxn* inactivation-induced molecular changes. A total of 3,561 genes are differentially expressed, among them one-third (1,235) are upregulated and two-thirds (2,326) are downregulated. Gene set enrichment analysis (GSEA) showed alteration in six signaling pathways enriched in $Lxn^{-/-}$ cells, and three of them involved cell-cell and cell-extracellular matrix interaction (Figure S2A). Among the top ten up- and downregulated genes (Figure S2B), *Thbs1* is one of the most interesting candidates. The rationale is that *Thbs1* is a multidomain matrix glycoprotein that interacts with numerous adhesion receptors and proteases, and mediates cell-cell and cell-matrix interactions (Adams and Lawler, 2011). *Thbs1* has been shown to enhance cell survival and regulate hematopoietic progenitor recovery under stress conditions (Isenberg et al., 2008). These functions are consistent with the functional effects of *Lxn* (You et al., 2014), which prompted us to further investigate whether *Thbs1* is the downstream target of *Lxn*. Our microarray data showed a significant decrease in *Thbs1* expression in $Lxn^{-/-}$ HSCs. Quantitative real-time PCR validated the downregulation of *Thbs1*; a reduction in mRNA expression of at least 2-fold was identified in different subsets of $Lxn^{-/-}$ HSCs (Figure 6A). It is noteworthy that the expression level of *Thbs1* increased with the content of primitive hematopoietic cells, reaching the highest in the most primitive HSC population. Such expression pattern is similar to that of *Lxn*, as we reported previously (Liang et al., 2007), further corroborating the association between *Thbs1* and *Lxn*. THBS1 protein, measured by western blot, also decreased in $Lxn^{-/-}$ HSC/HPC-enriched Lin– cKi+ cells (Figure 6B, left). THBS1 is a secreted protein (Adams and Lawler, 2011). We therefore measured its level in BM fluid and found that *Thbs1* content in the $Lxn^{-/-}$ BM microenvironment was also reduced (Figure 6B, right). Immunofluorescence staining of THBS1 protein level in BM sections of $Lxn^{-/-}$ mice confirmed reduced protein content of THBS1 (Figure 6C). Furthermore, Figure 6D shows that the THBS1 protein content was reduced in individual $Lxn^{-/-}$ LSK cells compared with WT ones (left), and the percentage

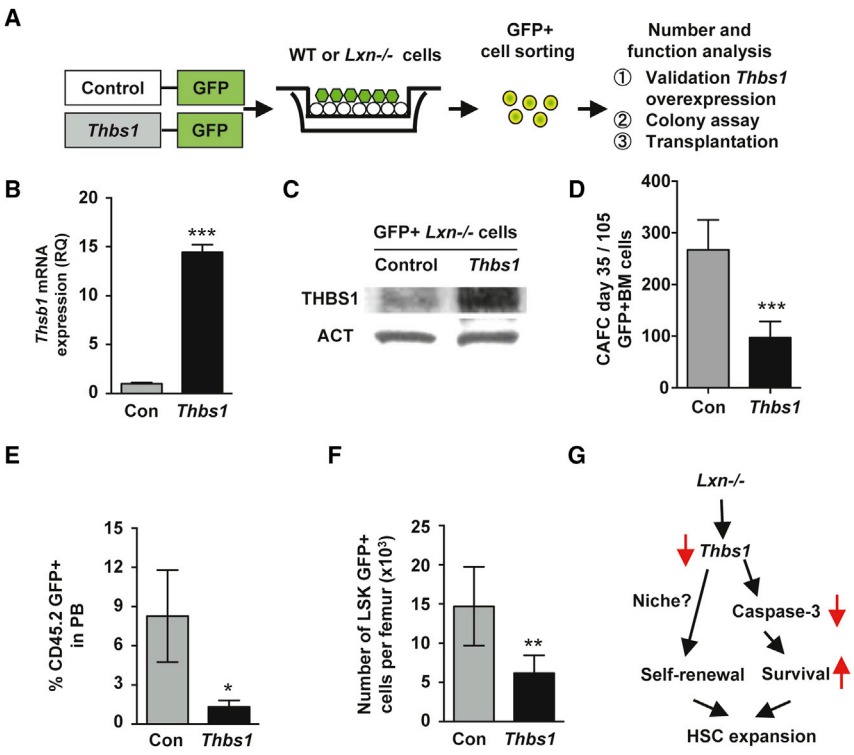

Figure 7. Overexpression *Thbs1* Rescues *Lxn*$^{-/-}$ Hematopoietic Phenotype

(A) Experimental scheme for lentivirus-mediated *Thbs1* overexpression strategy in LSK cells.

(B and C) Quantitative real-time PCR (B) and western blot analysis (C) of *Thbs1* mRNA and protein, respectively, in *Thbs1*-overexpressing (*Thbs1*) *Lxn*$^{-/-}$ LSK cells. Actin (ACT) was normalization control (Con). Blots are representative of two independent experiments. ***p < 0.001.

(D) Absolute number of HSC clones, defined by CAFC day 35 in *Thbs1*-overexpressing (*Thbs1*) *Lxn*$^{-/-}$ LSK cells. ***p < 0.001.

(E) Frequencies of *Thbs1*-overexpressing (*Thbs1*) or control *Lxn*$^{-/-}$ donor cells from (GFP+)-derived PB leukocytes in recipient mice. *p = 0.04.

(F) Absolute number of BM LSK cells, repopulated by *Thbs1* overexpression (*Thbs1*), or in control *Lxn*$^{-/-}$ donor cells (GFP+) from transplantation recipient mice. **p = 0.009. Presented data in (C–F) are the average ± SD pooled from two independent experiments with five recipients receiving GFP+ cells per experiment (n = 10 per donor group).

(G) Model of regulation of HSC function by the *Lxn-Thbs1* pathway. Deletion of the HSC regulatory gene, *Lxn*, causes downregulation of *Thbs1* mRNA and protein in stem cells, which may lead to the decreased level of active caspase-3. As a result, *Lxn*$^{-/-}$ HSCs have an enhanced survival. Decreased level of *Thbs1* in the BM environment may affect HSC-niche interaction, which may lead to the increased repopulating capacity of HSCs. Increased survival and function may contribute to the expansion of HSC pool.

of *Thbs1*+ LSK cells was significantly decreased in *Lxn*$^{-/-}$ BM cells compared with that in WT cells (right).

To further confirm the positive correlation between *Lxn* and *Thbs1* expression, we overexpressed *Lxn* in WT LSK cells, and found that *Thbs1* mRNA level was significantly increased (Figure S3). Moreover, we analyzed BM HSCs in *Thbs1*$^{+/-}$ mice in which THBS1 protein was decreased (Figure 6E), and found that the number of LSK cells and CAFC day 35 cells was significantly higher in *Thbs1*$^{+/-}$ BM than those in WT BM cells (Figures 6F and 6G), a phenotype similar to *Lxn*$^{-/-}$ mice (Figures 2D and 3A). These data strongly suggest that *Thbs1* is a downstream target of *Lxn*.

Thbs1 is a natural inhibitor of angiogenesis, megakaryopoiesis, and thrombopoiesis (Adams and Lawler, 2011), all of which have been shown as critical niche components implicated in HSC regulation (Kfoury and Scadden, 2015; Schepers et al., 2015; Bruns et al., 2014; Zhao et al., 2014), We asked whether the reduced *Thbs1* levels in *Lxn*$^{-/-}$ HSCs and surrounding environment could affect these niche components. There was no significant difference in the number of megakaryocytes and megakaryocyte progenitor cells in *Lxn*$^{-/-}$ mice (Figures S4A and S4B, respectively) compared with WT mice. No difference in the expression of von Willebrand factor and CD41, two megakaryocyte markers, was shown in the microarray of *Lxn*$^{-/-}$ cells (data not shown). Moreover, the number of endothelial cells and the function of platelets also remain unchanged in *Lxn*$^{-/-}$ mice (Figures S4C and S4D, respectively). Altogether, these data suggest that *Thbs1* is a specific downstream target of *Lxn*, and the decreased level of Thbs1 might affect *Lxn*$^{-/-}$ HSCs in a cell-intrinsic manner.

Enforced Expression of *Thbs1* Reverts the *Lxn*$^{-/-}$ HSC Phenotype

To directly address the involvement of *Thbs1* in the HSC phenotype of *Lxn*$^{-/-}$ mice, we overexpressed *Thbs1* in WT and Lxn$^{-/-}$ LSK cells (Figures 7A and S5). Quantitative real-time PCR and western blot analysis confirmed increased expression of *Thbs1* at both transcript and protein levels in *Lxn*$^{-/-}$ cells transduced with a *Thbs1* virus compared with cells transduced with empty vector (Figures 7B and 7C, respectively). Figure 7D showed that *Thbs1* overexpression dramatically reduced the number of *Lxn*$^{-/-}$ HSCs assessed by CAFC at day 35. Moreover, when *Thbs1*-overexpressing *Lxn*$^{-/-}$ stem cells were transplanted into myeloablated recipients, they showed a significant lower

capacity to reconstitute recipients' PB than control $Lxn^{-/-}$ cells at 16 weeks post transplantation (Figure 7E). Consistently, *Thbs1* overexpression reduced the BM LSK cell reconstitution by nearly 2-fold (Figure 7F), which reverted the increased repopulation capacity seen in $Lxn^{-/-}$ HSCs (Figures 3D and 3G). However, we did not see any significant change in CAFC day 35 number in *Thbs1*-overexpressing WT cells, suggesting *Thbs1* as a specific downstream target of *Lxn* (Figure S5). Overall, the data indicate that enforced *Thbs1* expression can revert the $Lxn^{-/-}$ phenotype, suggesting that the functional effect of *Lxn* may act, in part, through *Thbs1*.

DISCUSSION

Lxn was originally identified by the natural variation of HSC numbers between C57BL/6 and DBA/2 mice, in which the C57BL/6 strain had a lower HSC number than the DBA/2 strain (Liang et al., 2007). *Lxn* expression negatively correlates with this variation, that is, its expression is higher in C57BL/6 HSCs than DBA/2 stem cells. However, the specific role of *Lxn* in hematopoiesis remains largely unknown.

In this study, we determined the in vivo function of *Lxn* in regulating HSC function and maintaining homeostatic hematopoiesis, and uncovered the cellular and molecular mechanisms that control these processes. Using the *Lxn* knockout mouse model generated on the C57BL/6 background, we found that loss of *Lxn* in vivo led to an expansion of the entire hematopoietic hierarchy, from the stem cell pool to the PB cells. Very interestingly, the increased number of HSCs in $Lxn^{-/-}$ mice is comparable with that of the DBA/2 strain (Liang et al., 2007), suggesting that *Lxn*, as the natural regulator, has the unique characteristic of maintaining the physiologic range of the HSC pool size. Therefore, reduction or even deletion of *Lxn* activity results in a controlled expansion of HSCs without impairment of stem cell repopulating and multilineage differentiation capacity. Indeed, the transplantation studies show that $Lxn^{-/-}$ HSCs have a much better long-term repopulation capacity with a balanced output of blood cells. Moreover, controlled expansion reduces the risk of malignant hyperplasia, supported by the observation that $Lxn^{-/-}$ mice did not spontaneously develop hematologic malignancy even during aging. Altogether, antagonism of *Lxn* function may have a therapeutic potential through a controlled expansion of HSCs without exhaustion or transformation.

The molecular mechanisms by which *Lxn* regulates HSC function remain largely unknown. Here, we provide strong evidence to support Thbs1 as a downstream target that mediates control of HSC by *Lxn*: (1) loss of *Lxn* dramatically decreased *Thbs1* mRNA and protein levels; (2) ectopic expression of *Lxn* significantly increased *Thbs1* transcript level; (3) $Thbs1^{+/-}$ mice phenocopied $Lxn^{-/-}$ mice in their BM HSC population by showing an enlarged HSC pool; and (4) ectopic expression of *Thbs1* reverted the $Lxn^{-/-}$ HSC phenotype. *Thbs1* is a multidomain adhesive glycoprotein that mediates cell-cell and cell-matrix interactions (Adams and Lawler, 2011). It interacts with a wide range of cell adhesion receptors and numerous proteases, and is involved in various cellular processes, such as inhibition of angiogenesis, megakaryocytopoiesis, and platelet function (Yang et al., 2003; Kopp and Rafii, 2007; Isenberg et al., 2009). However, our results indicate that decreased expression and secretion of *Thbs*1 in $Lxn^{-/-}$ HSCs and surrounding environment does not alter these niche cellular components; Since *Thbs1* is a matrix protein, one of the regulatory mechanisms of *Lxn* may involve cell-cell and/or cell-niche interactions by altering the abundance of matrix proteins (Figure 7G). This discovery is consistent with a previous report from the Furukawa group, although they identified different adhesion molecules: N-cadherin, *Tie2*, and Roundabout 4 (Mitsunaga et al., 2012). This discrepancy may be due to the reasons that they used a less primitive cell population (SCA-1+) for proteomic analysis and/or they deleted the entire *Lxn* gene in the knockout mouse model. Nevertheless, additional investigations on the role of *Lxn* in stem cell trafficking, including mobilization and homing would be valuable.

Thbs1 can induce apoptosis via upregulation of active caspase-3 (Li et al., 2003). Consistently, $Lxn^{-/-}$ HSCs demonstrated decreased apoptosis and reduced levels of active caspase-3, suggesting that downregulation of *Thbs1* might also intrinsically enhance $Lxn^{-/-}$ stem cell survival (Figure 7G). An increased survival could boost stem cell tolerance to genotoxic or cytotoxic stress. Indeed, absence of *Thbs1* confers near complete resistance to injury from high-dose radiation, partly through mitigation of radiation-induced BM cell apoptosis (Isenberg et al., 2008; Soto-Pantoja et al., 2013). Moreover, *Thbs1* knockout mice demonstrated an accelerated hematopoietic recovery following 5-FU-induced myelosuppression (Kopp et al., 2006). Interestingly, our published work has shown that *Lxn* is involved in radiation response and it increases the radiation sensitivity of myeloid progenitor cells (You et al., 2014). Therefore, we speculate that loss of *Lxn* may protect HSCs from radiation- and/or chemotherapy-induced myelosuppression and long-term damages. We indeed showed that $Lxn^{-/-}$ mice had a much faster recovery in hematopoietic stem/progenitor cells from 5-FU-induced stress.

HSCs have served as a fundamental model for the study of stem cell biology and as a vital therapeutic modality for the treatment of hematopoietic malignancies and BM failure syndromes (Daley, 2012; Doulatov et al., 2012). Our results show that inhibition of *Lxn* activity leads to

the controlled expansion of HSC population without impairment of self-renewal capacity and induction of malignant hyperplasia. Therefore, *Lxn* might be a promising genetic target for HSC expansion. More importantly, since *Lxn* was identified by the genetic diversity underlying HSC natural variations, it is highly likely that *Lxn* may function similarly in humans and manipulation of *Lxn* activity could provide translational impact (Van Zant and Liang, 2009; Doulatov et al., 2012).

EXPERIMENTAL PROCEDURES

Animals

C57BL/6 mice and B6.SJL/BoyJ (CD45.1) recipient mice were purchased from The Jackson Laboratory. Latexin constitutive knockout mice ($Lxn^{-/-}$) were generated by TaconicArtemis. *Thbs1* heterozygous knockout mice ($Thbs1^{+/-}$) were kindly provided by Dr. Shuxia Wang (Li et al., 2016; Maimaitiyiming et al., 2016). All mice used were 8–12 weeks old. Mice were housed in the University of Kentucky animal facilities following NIH-mandated guidelines for animal welfare and with IACUC approval. Complete blood count was performed on a Hemavet 950 (Drew Scientific). 5-FU was intraperitoneally injected at a concentration of 100 mg/kg body weight.

Immunostaining and Flow Cytometry

HSCs, HPCs, and stromal cells: BM cells were stained with lineage antibodies, including CD5 (clone 53–7.3), CD8a (clone 53–6.7), CD45R/B220 (clone RA3-6B2), CD11b/MAC-1 (clone M1/70), LY-6G/GR-1 (clone RB6-8C5), and TER119/Ly-76 (clone TER-119)-APC-Cy7, and stem cell markers, C-KIT-APC, SCA-1-PE-Cy5.5, CD34-FITC, and FLT3-PE. HPCs were stained with FcγR and IL7R. HSC/HPC-enriched LSK cells, LT-HCSs and ST-HSCs, MPPs, and HPCs, including CMP, GMP, megakaryocyte/erythroid progenitor (MEP) and CLP cells were immunophenotypically defined as different markers. BM megakaryocytes and endothelial cells were stained with CD41 (clone MWR/REG30) and CD31 (clone MEC13.3), respectively. Dead cells were excluded by PI selection. PB lineage chimerism staining was stained with CD45.2 and CD45.1 markers and MAC-1/GR1, THY1, and B220 markers. Cell-cycle analysis was performed using Ki-67 and 7-aminoactinomycin D (7-AAD) staining. In vivo BrdU incorporation was used to study cell-cycle dynamics. BrdU was administered in drinking water (0.5 mg/mL) for 3 days and the percentage of BrdU+ LT-HSCs was analyzed daily. Apoptosis was performed with Annexin V and 7-AAD. Antibodies were purchased from eBioscience, BioLegend, or BD Pharmingen. Negative controls for fluorescence-activated cell sorting (FACS) gating was set by cells without any antibody staining. Flow cytometry was performed on a FACSAria II (Becton Dickinson) and the data were analyzed using FlowJo software (TreeStar).

In Vitro Colony Assays

(1) CFC assay was performed as described previously in complete MethoCult medium (STEMCELL Technologies), Colony formation was observed on days 7 and 14 (Liang et al., 2005). (2) CAFC assay was performed as described previously (Liang et al., 2007). The most primitive HSCs showed cobblestones at day 35, whereas HPCs show colonies at early dates, such as CAFC day 7. CAFC frequencies were calculated by using L-CaLc limiting dilution analysis software (STEMCELL Technologies).

BM Transplantation

In competitive repopulation assays, 1×10^6 donor cells from $Lxn^{-/-}$ or WT BM (CD45.2) mice were mixed with an equal number of competitor BM cells (B6.SJL/BoyJ) and retro-orbitally injected into lethally irradiated (9 Gy) recipient mice. For transplantation of *Thbs1*-overexpressing $Lxn^{-/-}$ cells, sorted 1×10^5 GFP+ cells that were either *Thbs-1* overexpression or empty vector control $Lxn^{-/-}$ BM cells were mixed with 2×10^5 competitor cells, and injected into B6.SJL/BoyJ recipient mice. Percentages of donor (CD45.2 or GFP+)-derived PB and BM cells were determined at 16 weeks post transplantation (Liang et al., 2007).

Microarray Analysis

Microarray was performed on LT-HSCs and MPPs in the Microarray Facility Center at the University of Kentucky. In brief, nearly 100,000 LT-HSCs and MPPs were sorted from pooled marrows of 10–20 WT or $Lxn^{-/-}$ mice. Total RNA was extracted using RNeasy Kit (QIAGEN) and processed onto the Affymetrix Gene Chip MoGene-1_0-st-v1 Arrays. Three independent samples were obtained from each strain. Microarray data were normalized by the robust multiarray averaging method. The limma package (Smyth, 2004) in R/Bioconductor was used to determine the differentially expressed genes. In GSEA (Subramanian et al., 2005) (www.broadinstitute.org/gsea/index.jsp), genes were preranked based on the absolute values of their limma test statistics. Pathways in the Kyoto Encyclopedia of Genes and Genomes database were investigated. Enriched pathways were identified with false discovery rate less than 0.2.

mRNA and Protein Quantification

Quantitative real-time PCR was performed as described previously (Liang et al., 2007) with a commercially available primer/probe mix for *Thbs1* in ABI PRISM 7700 (Applied Biosystems). Western blot was performed as described previously (Liang et al., 2007). Antibodies were anti-GFM-1 (Abcam), anti-THBS-1 (Cell Signaling Technology), anti-LXN, and anti-Actin (Sigma).

Overexpression of *Thbs-1* in BM Cells

Flow cytometry sorted LSK cells from C57/BL6 or $Lxn^{-/-}$ mice were stimulated with cytokines including 100 ng/mL FMS-like tyrosine kinase-3 ligand, 50 ng/mL mouse stem cell factor, 10 ng/mL interleukin-3 (IL-3), and 10 ng/mL IL-6 in StemSpan SFEM (STEMCELL Technologies). After 24 hr, the cells were transduced with lentiviral particles encoding either m*Thbs1* (catalog no. EX-Mm05712-Lv165), m*Lxn* (catalog no. EX-Mm03695-Lv165), or its related empty vector (catalog no. EX-NEG-Lv165), at an MOI of 100 for 6 hr at 37°C. All lentiviral particles were premade and purchased from GeneCopoeia. After 48 hr, the GFP-positive cells were sorted for real-time PCR, western blotting, CAFC assay, and transplantation assays. In transplantation assay, 1×10^5 GFP+ cells plus 2×10^5 competitor B6.SJL/BoyJ BM cells were injected into

B6.SJL/BoyJ mice, and GFP+ chimerism in PB and BM was measured at 16 weeks post transplantation. The CAFC assay of GFP+ cells was as described above.

Statistical Analysis

Data were examined for homogeneity of variances (F test), then analyzed by Welch's t test or one-way ANOVA with post hoc analysis by Tukey's test. Differences were considered significant at $p < 0.05$. All statistical analyses were conducted using SPSS 16.0 for Windows.

ACCESSION NUMBERS

The accession number for all microarray data reported in this paper is GEO: GSE94665.

SUPPLEMENTAL INFORMATION

Supplemental Information includes five figures and can be found with this article online at http://dx.doi.org/10.1016/j.stemcr.2017.02.009.

AUTHOR CONTRIBUTIONS

Experimentation, Y. Liu, C. Zhang, and Z.L.; Microarray Analysis, C.W. and J.L.; Technical Assistance on All Imaging Analysis, J.J.; Technical Assistance on Thbs1 Overexpression, T.G.; Insights on the Thbs1 Study, S.W.; Manuscript Review, S.B., D.St.C., D.Z., G.H., and C. Zhou; Pathological Analysis of Aged Mice, P.J.; Generation of Lxn Knockout Mice, H.G.; Study Design and Manuscript Preparation, Y. Liang.

ACKNOWLEDGMENTS

Research reported in this publication was supported by the National Heart, Lung, and Blood Institute of the NIH under Award Number RO1HL124015 (Y. Liang), the Edward P. Evans Foundation (S.B., D.S.C., D.Z., H.G., and Y. Liang), and the Biostatistics and Bioinformatics Shared Resource(s), Flow Cytometry Core of the University of Kentucky Markey Cancer Center (P30CA177558). We thank Carol Swiderski, Yanan You, and Rong Wen for technical assistance, and Garretson Epperly in the Imaging Core of the University of Kentucky Markey Cancer Center for confocal microscope imaging assistance, and the Markey Cancer Center's Research Communications Office for editing and graphics support.

Received: June 14, 2016
Revised: February 9, 2017
Accepted: February 10, 2017
Published: March 16, 2017

REFERENCES

Aagaard, A., Listwan, P., Cowieson, N., Huber, T., Ravasi, T., Wells, C.A., Flanagan, J.U., Kellie, S., Hume, D.A., Kobe, B., et al. (2005). An inflammatory role for the mammalian carboxypeptidase inhibitor latexin: relationship to cystatins and the tumor suppressor tig1. Structure *13*, 309–317.

Abd Elmageed, Z.Y., Moroz, K., and Kandil, E. (2013). Clinical significance of cd146 and latexin during different stages of thyroid cancer. Mol. Cell. Biochem. *381*, 95–103.

Abiola, O., Angel, J.M., Avner, P., Bachmanov, A.A., Belknap, J.K., Bennett, B., Blankenhorn, E.P., Blizard, D.A., Bolivar, V., Brockmann, G.A., et al. (2003). The nature and identification of quantitative trait loci: a community's view. Nat. Rev. Genet. *4*, 911–916.

Adams, J.C., and Lawler, J. (2011). The thrombospondins. Cold Spring Harb. Perspect. Biol. *3*, a009712.

Andrade, P.Z., dos Santos, F., Almeida-Porada, G., da Silva, C.L., and S. Cabral, J.M. (2010). Systematic delineation of optimal cytokine concentrations to expand hematopoietic stem/progenitor cells in co-culture with mesenchymal stem cells. Mol. Biosyst. *6*, 1207–1215.

Andrade, P.Z., da Silva, C.L., dos Santos, F., Almeida-Porada, G., and Cabral, J.M. (2011). Initial cd34+ cell-enrichment of cord blood determines hematopoietic stem/progenitor cell yield upon ex vivo expansion. J. Cell. Biochem. *112*, 1822–1831.

Antonchuk, J., Sauvageau, G., and Humphries, R.K. (2002). Hoxb4-induced expansion of adult hematopoietic stem cells ex vivo. Cell *109*, 39–45.

Avagyan, S., Aguilo, F., Kamezaki, K., and Snoeck, H.W. (2011). Quantitative trait mapping reveals a regulatory axis involving peroxisome proliferator-activated receptors, prdm16, transforming growth factor-beta2 and flt3 in hematopoiesis. Blood *118*, 6078–6086.

Blanpain, C., Daley, G.Q., Hochedlinger, K., Passegue, E., Rossant, J., and Yamanaka, S. (2012). Stem cells assessed. Nat. Rev. Mol. Cell Biol. *13*, 471–476.

Boitano, A.E., Wang, J., Romeo, R., Bouchez, L.C., Parker, A.E., Sutton, S.E., Walker, J.R., Flaveny, C.A., Perdew, G.H., Denison, M.S., et al. (2010). Aryl hydrocarbon receptor antagonists promote the expansion of human hematopoietic stem cells. Science *329*, 1345–1348.

Bruns, I., Lucas, D., Pinho, S., Ahmed, J., Lambert, M.P., Kunisaki, Y., Scheiermann, C., Schiff, L., Poncz, M., Bergman, A., et al. (2014). Megakaryocytes regulate hematopoietic stem cell quiescence through cxcl4 secretion. Nat. Med. *20*, 1315–1320.

Cahan, P., Li, Y., Izumi, M., and Graubert, T.A. (2009). The impact of copy number variation on local gene expression in mouse hematopoietic stem and progenitor cells. Nat. Genet. *41*, 430–437.

Chen, K.G., Mallon, B.S., McKay, R.D., and Robey, P.G. (2014). Human pluripotent stem cell culture: considerations for maintenance, expansion, and therapeutics. Cell Stem Cell *14*, 13–26.

Daley, G.Q. (2012). The promise and perils of stem cell therapeutics. Cell Stem Cell *10*, 740–749.

de Haan, G. (2007). Latexin is a newly discovered regulator of hematopoietic stem cells. Nat. Genet. *39*, 141–142.

Delaney, C., Heimfeld, S., Brashem-Stein, C., Voorhies, H., Manger, R.L., and Bernstein, I.D. (2010). Notch-mediated expansion of human cord blood progenitor cells capable of rapid myeloid reconstitution. Nat. Med. *16*, 232–236.

Doulatov, S., Notta, F., Laurenti, E., and Dick, J.E. (2012). Hematopoiesis: a human perspective. Cell Stem Cell *10*, 120–136.

Eaves, C.J. (2015). Hematopoietic stem cells: concepts, definitions, and the new reality. Blood *125*, 2605–2613.

Geiger, H., True, J.M., de Haan, G., and Van Zant, G. (2001). Age- and stage-specific regulation patterns in the hematopoietic stem cell hierarchy. Blood *98*, 2966–2972.

Goessling, W., Allen, R.S., Guan, X., Jin, P., Uchida, N., Dovey, M., Harris, J.M., Metzger, M.E., Bonifacino, A.C., Stroncek, D., et al. (2011). Prostaglandin e2 enhances human cord blood stem cell xenotransplants and shows long-term safety in preclinical nonhuman primate transplant models. Cell Stem Cell *8*, 445–458.

Goodell, M.A., Nguyen, H., and Shroyer, N. (2015). Somatic stem cell heterogeneity: diversity in the blood, skin and intestinal stem cell compartments. Nat. Rev. Mol. Cell Biol. *16*, 299–309.

Gottgens, B. (2015). Regulatory network control of blood stem cells. Blood *125*, 2614–2620.

Henckaerts, E., Geiger, H., Langer, J.C., Rebollo, P., Van Zant, G., and Snoeck, H.W. (2002). Genetically determined variation in the number of phenotypically defined hematopoietic progenitor and stem cells and in their response to early-acting cytokines. Blood *99*, 3947–3954.

Himburg, H.A., Muramoto, G.G., Daher, P., Meadows, S.K., Russell, J.L., Doan, P., Chi, J.T., Salter, A.B., Lento, W.E., Reya, T., et al. (2010). Pleiotrophin regulates the expansion and regeneration of hematopoietic stem cells. Nat. Med. *16*, 475–482.

Himburg, H.A., Harris, J.R., Ito, T., Daher, P., Russell, J.L., Quarmyne, M., Doan, P.L., Helms, K., Nakamura, M., Fixsen, E., et al. (2012). Pleiotrophin regulates the retention and self-renewal of hematopoietic stem cells in the bone marrow vascular niche. Cell Rep. *2*, 964–975.

Hsu, H.C., Lu, L., Yi, N., Van Zant, G., Williams, R.W., and Mountz, J.D. (2007). Quantitative trait locus (qtl) mapping in aging systems. Methods Mol. Biol. *371*, 321–348.

Huang, X., Shah, S., Wang, J., Ye, Z., Dowey, S.N., Tsang, K.M., Mendelsohn, L., Kato, G.J., Kickler, T., and Cheng, L. (2013). Extensive ex vivo expansion of functional human erythroid precursors established from umbilical cord blood cells by defined factors. Mol. Ther. *22*, 451–463.

Isenberg, J.S., Maxhimer, J.B., Hyodo, F., Pendrak, M.L., Ridnour, L.A., DeGraff, W.G., Tsokos, M., Wink, D.A., and Roberts, D.D. (2008). Thrombospondin-1 and cd47 limit cell and tissue survival of radiation injury. Am. J. Pathol. *173*, 1100–1112.

Isenberg, J.S., Martin-Manso, G., Maxhimer, J.B., and Roberts, D.D. (2009). Regulation of nitric oxide signalling by thrombospondin 1: implications for anti-angiogenic therapies. Nat. Rev. Cancer *9*, 182–194.

Jordan, C.T., and Van Zant, G. (1998). Recent progress in identifying genes regulating hematopoietic stem cell function and fate. Curr. Opin. Cell Biol. *10*, 716–720.

Kfoury, Y., and Scadden, D.T. (2015). Mesenchymal cell contributions to the stem cell niche. Cell Stem Cell *16*, 239–253.

Kopp, H.G., and Rafii, S. (2007). Thrombopoietic cells and the bone marrow vascular niche. Ann. N. Y. Acad. Sci. *1106*, 175–179.

Kopp, H.G., Hooper, A.T., Broekman, M.J., Avecilla, S.T., Petit, I., Luo, M., Milde, T., Ramos, C.A., Zhang, F., Kopp, T., et al. (2006). Thrombospondins deployed by thrombopoietic cells determine angiogenic switch and extent of revascularization. J. Clin. Invest. *116*, 3277–3291.

Kunisaki, Y., and Frenette, P.S. (2012). The secrets of the bone marrow niche: enigmatic niche brings challenge for hsc expansion. Nat. Med. *18*, 864–865.

Lechman, E.R., Gentner, B., van Galen, P., Giustacchini, A., Saini, M., Boccalatte, F.E., Hiramatsu, H., Restuccia, U., Bachi, A., Voisin, V., et al. (2012). Attenuation of mir-126 activity expands hsc in vivo without exhaustion. Cell Stem Cell *11*, 799–811.

Li, K., Yang, M., Yuen, P.M., Chik, K.W., Li, C.K., Shing, M.M., Lam, H.K., and Fok, T.F. (2003). Thrombospondin-1 induces apoptosis in primary leukemia and cell lines mediated by cd36 and caspase-3. Int. J. Mol. Med. *12*, 995–1001.

Li, Y., Basang, Z., Ding, H., Lu, Z., Ning, T., Wei, H., Cai, H., and Ke, Y. (2011). Latexin expression is downregulated in human gastric carcinomas and exhibits tumor suppressor potential. BMC Cancer *11*, 121.

Li, Y., Turpin, C.P., and Wang, S. (2016). Role of thrombospondin 1 in liver diseases. Hepatol. Res. http://dx.doi.org/10.1111/hepr.12787.

Liang, Y., Van Zant, G., and Szilvassy, S.J. (2005). Effects of aging on the homing and engraftment of murine hematopoietic stem and progenitor cells. Blood *106*, 1479–1487.

Liang, Y., Jansen, M., Aronow, B., Geiger, H., and Van Zant, G. (2007). The quantitative trait gene latexin influences the size of the hematopoietic stem cell population in mice. Nat. Genet. *39*, 178–188.

Liu, Q., Yu, L., Gao, J., Fu, Q., Zhang, J., Zhang, P., Chen, J., and Zhao, S. (2000). Cloning, tissue expression pattern and genomic organization of latexin, a human homologue of rat carboxypeptidase A inhibitor. Mol. Biol. Rep. *27*, 241–246.

Liu, Y., Howard, D., Rector, K., Swiderski, C., Brandon, J., Schook, L., Mehta, J., Bryson, J.S., Bondada, S., and Liang, Y. (2012). Latexin is down-regulated in hematopoietic malignancies and restoration of expression inhibits lymphoma growth. PLoS One *7*, e44979.

Maimaitiyiming, H., Zhou, Q., and Wang, S. (2016). Thrombospondin 1 deficiency ameliorates the development of adriamycin-induced proteinuric kidney disease. PLoS One *11*, e0156144.

Mitsunaga, K., Kikuchi, J., Wada, T., and Furukawa, Y. (2012). Latexin regulates the abundance of multiple cellular proteins in hematopoietic stem cells. J. Cell. Physiol. *227*, 1138–1147.

Mouradov, D., Craven, A., Forwood, J.K., Flanagan, J.U., Garcia-Castellanos, R., Gomis-Ruth, F.X., Hume, D.A., Martin, J.L., Kobe, B., and Huber, T. (2006). Modelling the structure of latexin-carboxypeptidase a complex based on chemical cross-linking and molecular docking. Protein Eng. Des. Sel. *19*, 9–16.

Muthusamy, V., Premi, S., Soper, C., Platt, J., and Bosenberg, M. (2013). The hematopoietic stem cell regulatory gene latexin has tumor-suppressive properties in malignant melanoma. J. Invest. Dermatol. *133*, 1827–1833.

Nathan, D.G., and Orkin, S.H. (2009). Musings on genome medicine: genome wide association studies. Genome Med. *1*, 3.

Ni, Q.F., Tian, Y., Kong, L.L., Lu, Y.T., Ding, W.Z., and Kong, L.B. (2014). Latexin exhibits tumor suppressor potential in hepatocellular carcinoma. Oncol. Rep. *31*, 1364–1372.

Pallares, I., Bonet, R., Garcia-Castellanos, R., Ventura, S., Aviles, F.X., Vendrell, J., and Gomis-Ruth, F.X. (2005). Structure of human carboxypeptidase a4 with its endogenous protein inhibitor, latexin. Proc. Natl. Acad. Sci. USA *102*, 3978–3983.

Rossi, L., Lin, K.K., Boles, N.C., Yang, L., King, K.Y., Jeong, M., Mayle, A., and Goodell, M.A. (2012). Less is more: unveiling the functional core of hematopoietic stem cells through knockout mice. Cell Stem Cell *11*, 302–317.

Sankaran, V.G., and Orkin, S.H. (2013). Genome-wide association studies of hematologic phenotypes: a window into human hematopoiesis. Curr. Opin. Genet. Dev. *23*, 339–344.

Schepers, K., Campbell, T.B., and Passegue, E. (2015). Normal and leukemic stem cell niches: insights and therapeutic opportunities. Cell Stem Cell *16*, 254–267.

Smyth, G.K. (2004). Linear models and empirical Bayes methods for assessing differential expression in microarray experiments. Stat. Appl. Genet. Mol. Biol. *3*, Article3.

Soto-Pantoja, D.R., Ridnour, L.A., Wink, D.A., and Roberts, D.D. (2013). Blockade of cd47 increases survival of mice exposed to lethal total body irradiation. Sci. Rep. *3*, 1038.

Subramanian, A., Tamayo, P., Mootha, V.K., Mukherjee, S., Ebert, B.L., Gillette, M.A., Paulovich, A., Pomeroy, S.L., Golub, T.R., Lander, E.S., et al. (2005). Gene set enrichment analysis: a knowledge-based approach for interpreting genome-wide expression profiles. Proc. Natl. Acad. Sci. USA *102*, 15545–15550.

Uratani, Y., Takiguchi-Hayashi, K., Miyasaka, N., Sato, M., Jin, M., and Arimatsu, Y. (2000). Latexin, a carboxypeptidase A inhibitor, is expressed in rat peritoneal mast cells and is associated with granular structures distinct from secretory granules and lysosomes. Biochem. J. *3*, 817–826.

Van Zant, G., and Liang, Y. (2009). Natural genetic diversity as a means to uncover stem cell regulatory pathways. Ann. N. Y. Acad. Sci. *1176*, 170–177.

Walasek, M.A., van Os, R., and de Haan, G. (2012). Hematopoietic stem cell expansion: challenges and opportunities. Ann. N. Y. Acad. Sci. *1266*, 138–150.

Yang, M., Li, K., Ng, M.H., Yuen, P.M., Fok, T.F., Li, C.K., Hogg, P.J., and Chong, B.H. (2003). Thrombospondin-1 inhibits in vitro megakaryocytopoiesis via cd36. Thromb. Res. *109*, 47–54.

You, Y., Wen, R., Pathak, R., Li, A., Li, W., St Clair, D., Hauer-Jensen, M., Zhou, D., and Liang, Y. (2014). Latexin sensitizes leukemogenic cells to gamma-irradiation-induced cell-cycle arrest and cell death through rps3 pathway. Cell Death Dis. *5*, e1493.

Zhao, M., Perry, J.M., Marshall, H., Venkatraman, A., Qian, P., He, X.C., Ahamed, J., and Li, L. (2014). Megakaryocytes maintain homeostatic quiescence and promote post-injury regeneration of hematopoietic stem cells. Nat. Med. *20*, 1321–1326.

Zheng, J., Umikawa, M., Cui, C., Li, J., Chen, X., Zhang, C., Hyunh, H., Kang, X., Silvany, R., Wan, X., et al. (2012). Inhibitory receptors bind ANGPTLs and support blood stem cells and leukaemia development. Nature *485*, 656–660.

Stem Cell Reports, Volume *8*

Supplemental Information

Latexin Inactivation Enhances Survival and Long-Term Engraftment of Hematopoietic Stem Cells and Expands the Entire Hematopoietic System in Mice

Yi Liu, Cuiping Zhang, Zhenyu Li, Chi Wang, Jianhang Jia, Tianyan Gao, Gerhard Hildebrandt, Daohong Zhou, Subbarao Bondada, Peng Ji, Daret St. Clair, Jinze Liu, Changguo Zhan, Hartmut Geiger, Shuxia Wang, and Ying Liang

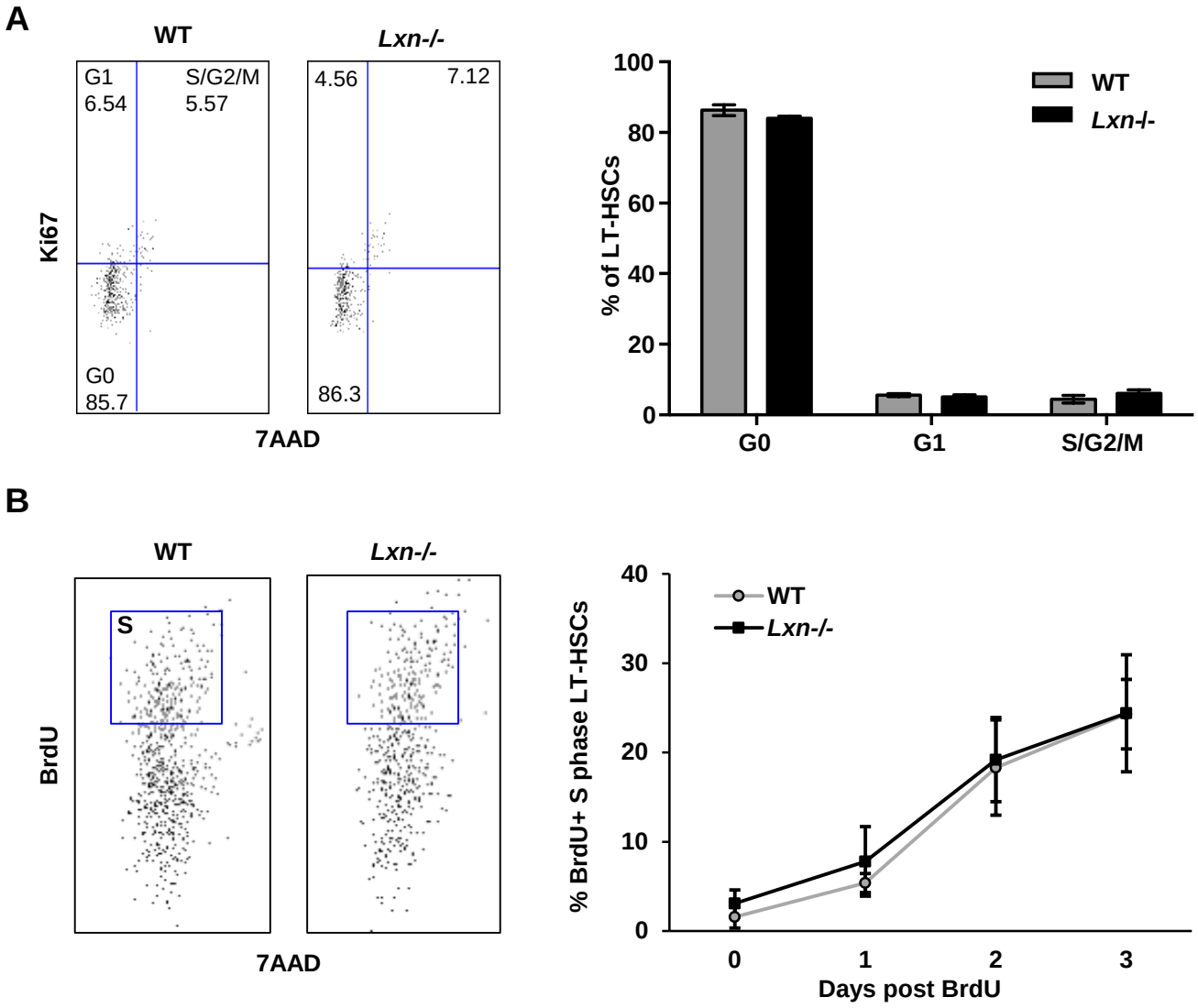

Supplementary Figure 1

Supplementary Figure 1.*Lxn* deletion does not alter HSC proliferation.
(**A**) Representative FACS plots showing the G0 (Ki67- and 7AAD-), G1 (Ki67+ and 7AAD-), and S/G2/M (Ki67+and 7AAD+) cell cycle phases in *Lxn-/-* and WT LT-HSCs (Lin-Sca1+c-Kit+CD34-Flt2- cells (left panel). The right panel shows the frequencies of each phase presented as the average ± SD of 6 measurements from 2 independent experiments. (**B**) Representative FACS plots showing proliferating S phase cells that are positive for BrdU incorporation. Right panel shows the accumulation of cycling *Lxn-/-* and WT LT-HSCs (BrdU+) over 3 days. Presented data are the average ± SD of 2 independent experiments, each performed with 3 mice (n=6).

A **Top functional categories significantly enriched in *Lxn-/-* HSCs**

Functional Categories	FDR q-val	# of Genes in Leading Edge
Neuroactive Ligand Receptor Interaction	0.002	147
Cell Communication	0.003	88
Proteasome	0.004	14
Arachidonic Acid Metabolism	0.120	42
Systemic Lupus Erythematosus	0.143	66
ECM Receptor Interaction	0.188	44

B **Top 10 genes significantly downregulated or upregulated in *Lxn-/-* HSCs**

Downregulated	Upregulated
Xist	*Kdm5d*
Thbs1	*Hspa1a/Hspa1B*
Pgr	*Rnase3*
Trpc6	*Tsen15*
Slc18a2	*Gas5*
Gfi1b	*Hsph1*
Kir3dl2	*Mrpl18*
Slc35d3	*Trem1*
Prkaa2	*Ccr2*
Homx1	*Cspp1*

Supplementary Figure 2

Supplementary Figure 2. Genes and functional categories altered in *Lxn-/-* HSCs.
(A) Functional categories of genes dysregulated in *Lxn-/-* LT-HSCs and MPPs identified by GSEA based on microarray data with false discovery rate (FDR)<0.2. The FDR q value and the number of genes in the leading edge subset for each category are also presented.
(B) Top ten genes that are significantly up-regulated or down-regulated in *Lxn-/-* HSCs.

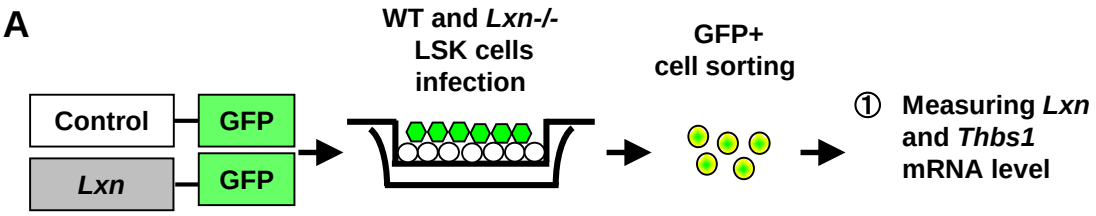

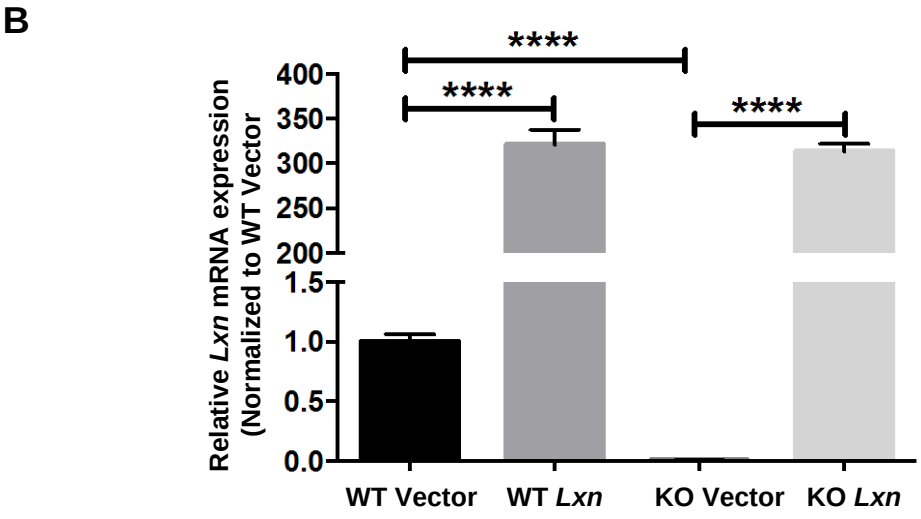

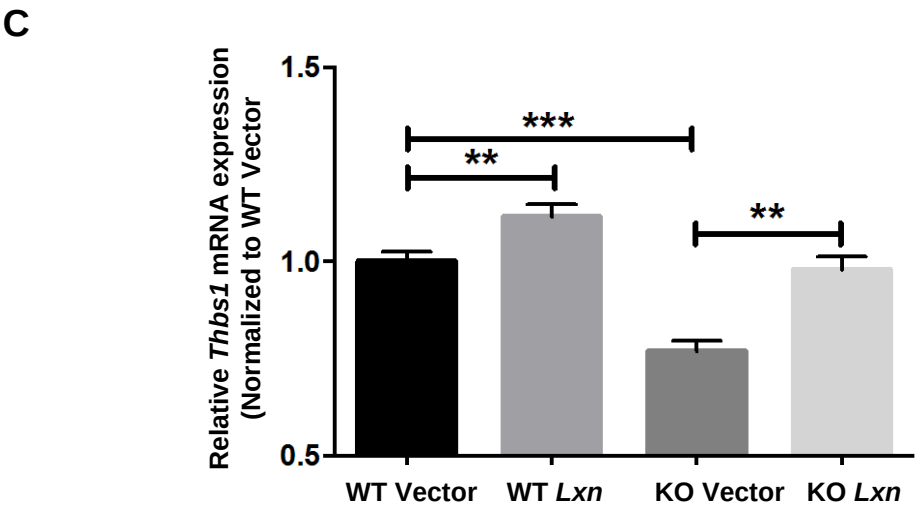

Supplementary Figure 3

Supplementary Figure 3. Increased expression of *Thbs1* in *Lxn*-overexpressing LSK cells.
(A) Experimental scheme for lentivirus-mediated *Lxn* overexpression strategy in WT and *Lxn-/-* LSK cells. WT or *Lxn-/-* LSK cells were sorted and transduced with empty control or *Lxn*-containing lentiviral particles. Successfully transduced cells were sorted by GFP expression, and *Lxn* and *Thbs*1 mRNA levels were measured by Real-time quantitative PCR. **(B)** Confirmation of increased *Lxn* mRNA level in WT and *Lxn-/-* LSK cells overexpressing *Lxn*. **(C)** *Thbs1* expression was significantly increased in WT and *Lxn-/-* LSK cells overexpressing *Lxn.* Data shown are Mean ± SD of 3 replicates. **** indicates p value <0.0001, *** indicates p value <0.001, and ** indicate p value < 0.01.

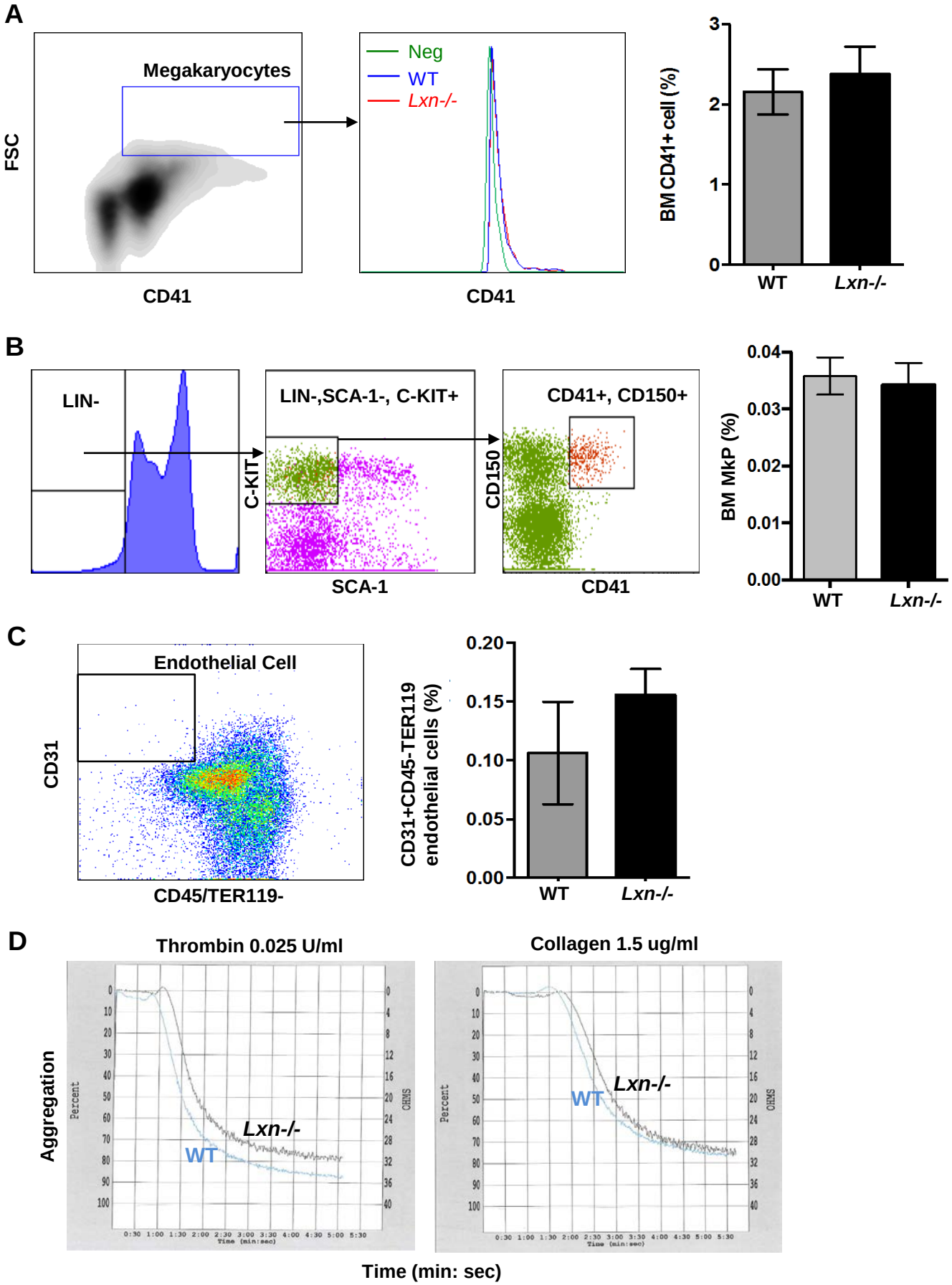

Supplementary Figure 4

Supplementary Figure 4. *Lxn* deletion does not alter BM niche components and platelet function.

(A) Representative FACS plot showing the identification of CD41+ FSC^{high} megakaryocytes (MKs) (left panel). No difference in the CD41 expression in the histogram of MK cells (middle panel), or in the percentage of MK cells (right panel) between BM MKs from *Lxn-/-* and WT was observed. Neg represents unstained negative control. **(B)** Representative FACS plot showing megakaryocyte progenitor cells (MkPs) that are identified as LIN-, SCA-1-, C-KIT+, CD41+, CD150+ cells (left panel). No difference was shown in the percentage of MkP cells between *Lxn-/-* and WT BMs (right panel). **(C)** Representative FACS plot showing the identification of CD31+CD45-Ter119- endothelial cells in the BM (left panel). No difference was observed in the percentage of BM endothelial cells between *Lxn-/-* and WT mice. **(D)** Measurement of platelet aggregation and secretion in response to agonists, thrombin (left) and collagen (right). Whole blood was collected from the inferior vena cava using one-seventh volume of ACD (85mM trisodium citrate, 83mM dextrose, and 21mM citric acid) as anticoagulant. Platelets were washed twice with CGS (0.12M NaCl, 0.0129M trisodium citrate, and 0.03M D-glucose, pH 6.5), resuspended in modified Tyrode's buffer at $3x10^8$/ml, and incubated for 2h at 22°C before use. Luciferin/luciferase reagent (12ml) was added to 238ml of washed platelet suspension within 1min before stimulation. Platelet aggregation and secretion were elicited by adding platelet agonists and recorded in real time in a Chrono-log lumiaggregometer at 37°C with stirring (1000 rpm). No difference in platelet aggregation between $Lxn^{-/-}$ and WT platelets was observed. Data shown are the Mean ± SD of 3 independent replicates.

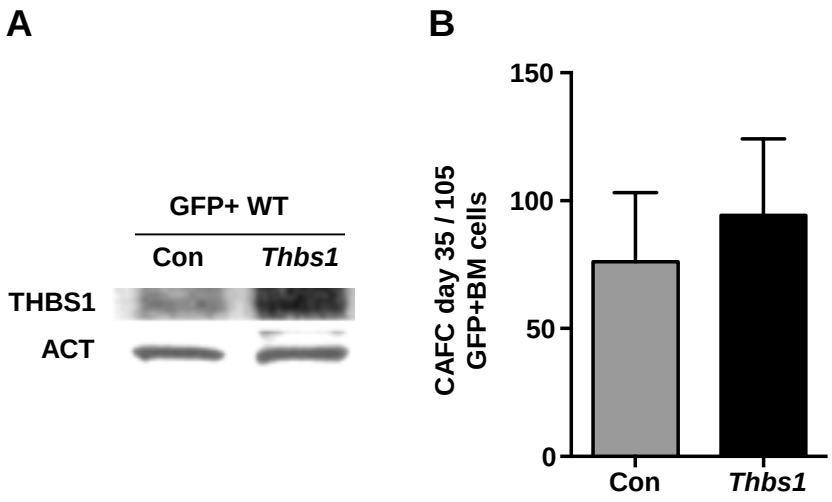

Supplementary Figure 5

Supplementary Figure 5. Overexpression *Thbs1* did not affect WT HSC number
(A) *Thbs1* was overexpressed in WT LSK cells using same strategy shown in **Figure 7A**. Western blot analysis of THBS1 protein in *Thbs1*-overexpressing (*Thbs1*) WT LSK cells. Actin (ACT) was the internal normalization control. Blots are representative of 2 independent experiments. **(B)** Absolute number of HSC clones, defined by cobblestone area forming cell (CAFC) assay, at d35 of culture in *Thbs1*-overexpressing (*Thbs1*) WT LSK cells.